

Transformation of electrical transport from variable range hopping to hard gap resistance in $\text{Zn}_{1-x}\text{Fe}_x\text{O}_{1-v}$ magnetic semiconductor films

Y. F. Tian,^{a)} Shi-shen Yan, Y. P. Zhang, H. Q. Song, G. Ji, G. L. Liu, Y. X. Chen, and L. M. Mei

School of Physics and Microelectronics, Shandong University, Jinan, Shandong 250100, People's Republic of China and National Key Laboratory of Crystal Materials, Shandong University, Jinan, Shandong, 250100, People's Republic of China

J. P. Liu, B. Altunçevahir, and V. Chakka

Department of Physics, The University of Texas at Arlington, P.O. Box 19059, Arlington, Texas 76019

(Received 18 February 2006; accepted 30 August 2006; published online 16 November 2006)

Transformation of the electrical transport from the Efros and Shklovskii [J. Phys. C **8**, L49 (1975)] variable range hopping to the “hard gap” resistance was experimentally observed in a low temperature range as the Fe compositions in $\text{Zn}_{1-x}\text{Fe}_x\text{O}_{1-v}$ ferromagnetic semiconductor films increase. A universal form of the resistance versus temperature, i.e., $\rho \propto \exp[T_H/T + (T_{ES}/T)^{1/2}]$, was theoretically established to describe the experimental transport phenomena by taking into account the electron-electron Coulomb interaction, spin-spin exchange interaction, and hard gap energy. The spin polarization ratio, hard gap energy, and ratio of exchange interaction to Coulomb interaction were obtained by fitting the theoretical model to the experimental results. Moreover, the experimental magnetoresistance was also explained by the electrical transport model. © 2006 American Institute of Physics. [DOI: [10.1063/1.2386925](https://doi.org/10.1063/1.2386925)]

I. INTRODUCTION

Various electrical transport phenomena in disordered systems^{1–20} have been extensively studied due to the significant importance not only in fundamental physics but also in technological applications. Assuming that the density of state is a constant near the Fermi energy, the variable range hopping resistance,¹ $\rho \propto \exp[(T_M/T)^{1/4}]$, was predicted by Mott for the disordered systems without Coulomb interaction. The Efros and Shklovskii variable range hopping model,² $\rho \propto \exp[(T_{ES}/T)^{1/2}]$, was proposed for a system of long range electron-electron Coulomb interaction. The “hard gap” resistance,^{3–8,11,12} $\rho \propto \exp(T_H/T)$, was observed in low temperature range in some systems with a hard gap in the density of state.

The transformation from the Efros variable range hopping to the hard gap resistance was observed in some materials as temperature decreases, and several models were proposed to explain the formation of the hard gap. In amorphous $\text{Ge}_{1-x}\text{Cr}_x$ (Ref. 12) and insulating Si:B,⁷ the hard gap energy was believed to originate from spin-spin exchange interaction after spin-glass ordering. In amorphous In/InO_x films, the hard gap was interpreted in terms of electric polaron excitations^{3,10} due to many-electron interactions. In dilute magnetic material $\text{Cd}_{1-x}\text{Mn}_x\text{Te}:\text{In}$, the hard gap was explained by the formation of magnetic polarons.⁴

For most doped nonmagnetic semiconductors, magnetoresistance was usually found at low temperature, and several mechanisms of magnetoresistance were proposed.^{13–20} Generally speaking, the electrical transport in the Anderson localization region is usually through the variable range hopping, and the magnetoresistance in doped semiconductors

can originate from orbital effects¹³ and spin effects.^{14–20} It is worthy to mention that the above investigations of electrical transport and magnetoresistance were mainly done on the nonferromagnetic disordered semiconductor system.

However, for ferromagnetic semiconductors with spin-polarized carriers, the electrical transport properties are influenced by not only Coulomb interactions between charges of the electrons but also exchange interactions between spins of the electrons. To date, there is not a quantitative theoretical electrical transport model of ferromagnetic semiconductors, which has taken into account the spin polarization, Coulomb interaction, and exchange interaction in the same frame. In addition, it is unknown if there exists a hard gap in ferromagnetic semiconductors. In this paper, we first reported the experimental results of the transformation from the variable range hopping to the hard gap resistance in the $\text{Zn}_{1-x}\text{Fe}_x\text{O}_{1-v}$ ($0 < x < 1$, and v means the vacancy of O atoms) ferromagnetic semiconductor, and then established a theoretical model to give a universal description of the electrical transport phenomena by taking into account electron-electron Coulomb interaction, spin-spin exchange interaction, and hard gap energy in the same frame. Moreover, the experimental magnetoresistance was also explained by the electrical transport model.

II. EXPERIMENT

$\text{Zn}_{1-x}\text{Fe}_x\text{O}_{1-v}$ magnetic semiconductor films with different compositions were prepared on glass substrates in a flow of Ar gas and remanent low O₂ background at room temperature. $\text{Zn}_{1-x}\text{Fe}_x\text{O}_{1-v}$ single layer films were formed by controlling atomic interdiffusion between the alternately deposited Fe and ZnO bilayers of a few angstroms for 30 periods. During each period, the Fe layer was deposited by dc mag-

^{a)}Electronic mail: yufengtian@hotmail.com

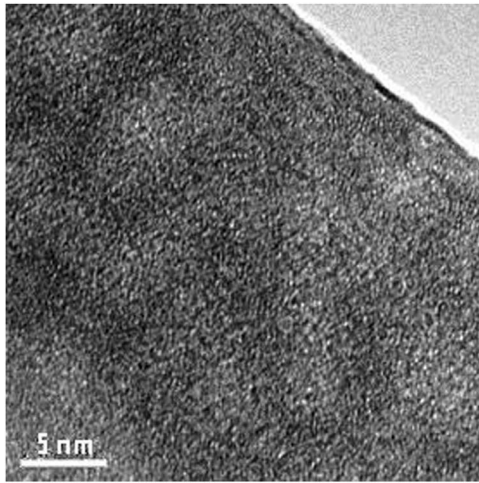


FIG. 1. A TEM image of the as-deposited $\text{Zn}_{0.3}\text{Fe}_{0.7}\text{O}_{1-v}$ film in the cross section view.

neutron sputtering at a growth rate of 0.30 \AA/s and its thickness was fixed at 4.9 \AA ; the ZnO layer was deposited by rf sputtering at a growth rate of 0.15 \AA/s and its thickness varied from 1.4 to 12 \AA . The detailed preparation process is similar to that used in Ref. 21.

The as-prepared $\text{Zn}_{1-x}\text{Fe}_x\text{O}_{1-v}$ samples are single layer amorphous films, which were observed by transmission electron microscope (TEM) in a cross section view. Figure 1 is a TEM image of the as-deposited $\text{Zn}_{0.3}\text{Fe}_{0.7}\text{O}_{1-v}$ film in the cross section view. It is clear that the film is in an amorphous state. The weak and uniform contrast indicates that compositions of the cross section are nearly uniform on a large scale. Further studies indicate that the chemical compositions of the $\text{Zn}_{1-x}\text{Fe}_x\text{O}_{1-v}$ samples are inhomogeneous on the subnanometer scale, but no pure Fe metal clusters were found within the films. The ferromagnetism with Curie temperature above room temperature was found by superconducting quantum interference device (SQUID) measurements. Electrical transport properties were measured in a Von der Pawn configuration by physical property measurement system (PPMS). The magnetic field was applied in plane of the film for magnetic and electrical transport measurements.

III. EXPERIMENTAL RESULTS

Figures 2(a)–2(c) show the temperature dependence of $\ln \rho$ vs T^α ($-1 \leq \alpha < 0$, ρ is sheet resistance and T is temperature) in magnetic field and without field for the $\text{Zn}_{1-x}\text{Fe}_x\text{O}_{1-v}$ films of different compositions. The solid lines in Figs. 2(a)–2(c) are the theoretical fittings to the experimental data according to $\ln \rho = B + CT^\alpha$, where B and C are two fitting coefficients for a given α value. Figure 2(a) ($\text{Zn}_{0.3}\text{Fe}_{0.7}\text{O}_{1-v}$) shows a good linear relation of $\ln \rho$ vs $T^{-1/2}$ in a wide temperature range, which is the Efros and Shklovskii variable range hopping resistance. For samples with lower Fe compositions, such as $\text{Zn}_{0.5}\text{Fe}_{0.5}\text{O}_{1-v}$ and $\text{Zn}_{0.54}\text{Fe}_{0.46}\text{O}_{1-v}$, their resistance also obeys the Efros and Shklovskii variable range hopping theory in a wide temperature range (figures are not shown here). Figure 2(c) ($\text{Zn}_{0.14}\text{Fe}_{0.86}\text{O}_{1-v}$) shows a linear relation of $\ln \rho$ vs T^{-1} in a low temperature range, i.e., the simple thermal activation form of the resistance, which is a

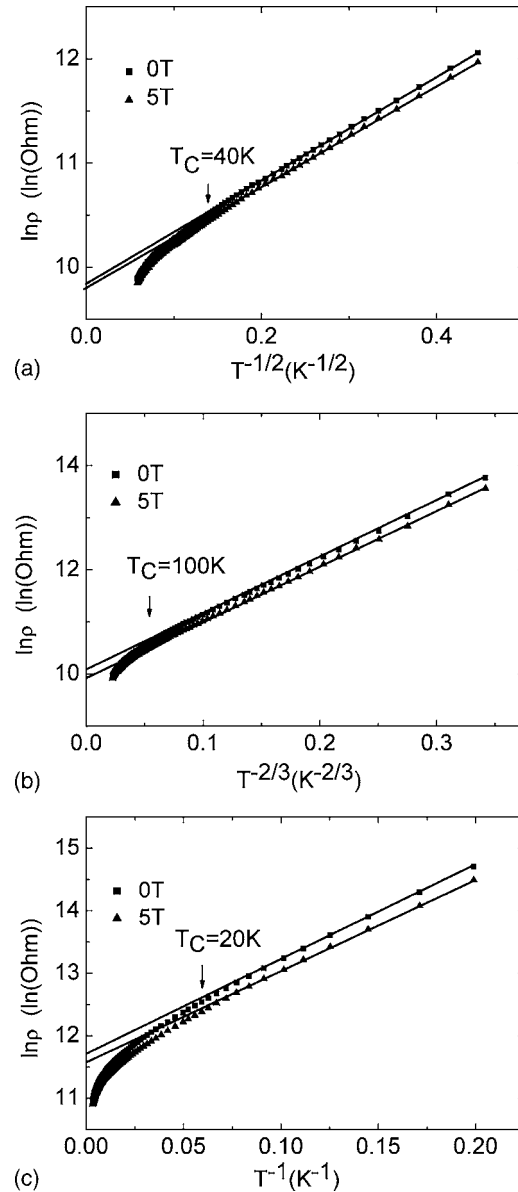


FIG. 2. The dependence of $\ln \rho$ on T^α for $\text{Zn}_{1-x}\text{Fe}_x\text{O}_{1-v}$ magnetic semiconductors with different Fe compositions, i.e., (a) $\text{Zn}_{0.3}\text{Fe}_{0.7}\text{O}_{1-v}$, (b) $\text{Zn}_{0.23}\text{Fe}_{0.77}\text{O}_{1-v}$, and (c) $\text{Zn}_{0.14}\text{Fe}_{0.86}\text{O}_{1-v}$. Squares and triangles are the experimental data in the demagnetized state ($H=0$) and in the saturation state ($H=5 \text{ T}$), respectively. The solid lines were theoretical fittings by $\ln \rho = B + CT^\alpha$ (see the text). The mark T_C is a temperature below which the experimental results can be well described by $\ln \rho = B + CT^\alpha$ for given samples.

manifestation of the existence of a hard gap in the density of state near the Fermi energy. Figure 2(b) ($\text{Zn}_{0.23}\text{Fe}_{0.77}\text{O}_{1-v}$) reveals a good linear relation of $\ln \rho$ vs $T^{-2/3}$. From Figs. 2(a)–2(c), it is clear that electrical transport mechanisms in the low temperature range transform from the variable range hopping to the hard gap resistance as the Fe composition increases in the $\text{Zn}_{1-x}\text{Fe}_x\text{O}_{1-v}$ magnetic semiconductor, which is different from the crossover of the electrical transport caused by temperature change.^{4–7}

More interestingly, the $\ln \rho$ vs T^α curves in magnetic field and without field are both straight lines in the low temperature range, but the theoretical fitting straight lines have different slopes and intersections. This means that the external magnetic field does not change the electrical transport

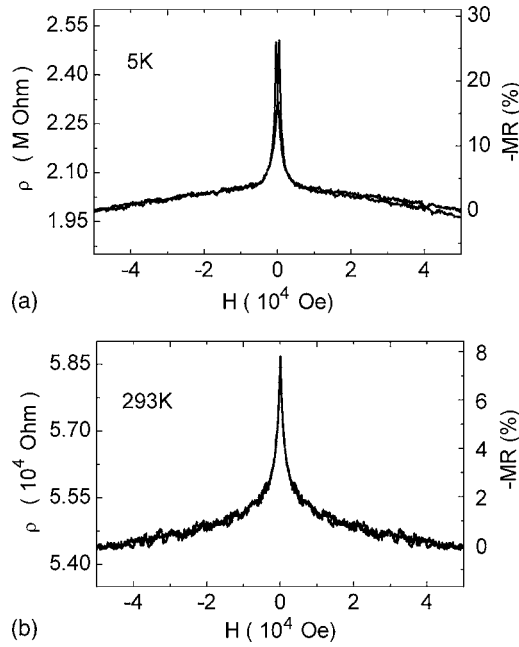


FIG. 3. The magnetic field dependence of the sheet resistance and the magnetoresistance for the sample $\text{Zn}_{0.14}\text{Fe}_{0.86}\text{O}_{1-v}$.

mechanisms but it can induce large magnetoresistance. Figure 3 shows the magnetic field dependence of the sheet resistance ρ and the magnetoresistance of the $\text{Zn}_{0.14}\text{Fe}_{0.86}\text{O}_{1-v}$ film. The magnetoresistance ratio is about 27% at 5 K and 8% at 293 K.

IV. THEORETICAL MODEL OF ELECTRICAL TRANSPORT

It is natural to expect that both the variable range hopping and the hard gap mechanisms may contribute to the electrical transport of $\text{Zn}_{1-x}\text{Fe}_x\text{O}_{1-v}$ magnetic semiconductor films. Based on this idea, a universal form of the resistance versus temperature was derived, i.e.,

$$\ln \rho = \ln \left(\frac{\rho_0}{1 + P^2 \langle \cos \theta \rangle} \right) + \frac{T_H}{T} + \left(\frac{\langle T_{ES} \rangle}{T} \right)^{1/2}, \quad (1)$$

which can well describe the observed experimental results.

Following the work in Refs. 19 and 22 on the hopping resistance in disordered systems and taking into account the influence of the spin polarization ratio on tunneling resistance,^{23,24} the hopping resistance (ρ_{ij}) between two localized states i and j of an energy difference ε_{ij} is given as

$$\rho_{ij} = \frac{\rho_0}{1 + P^2 \cos \theta} \exp(2r/\xi + \varepsilon_{ij}/k_B T), \quad (2)$$

where $r = |\mathbf{r}_i - \mathbf{r}_j|$ is the distance between the initial i state and the final j state in real space, ξ is the localization length, P is the spin polarization ratio of the carriers near the Fermi level, θ is the angle between the spin \mathbf{S}_i in the i state and \mathbf{S}_j in the j state at the distance r , ρ_0 is a resistance prefactor, and k_B is the Boltzmann constant. The transport properties are mainly determined by the energy difference ε_{ij} between the initial occupied i state and the final vacant j state of the hopping process. As ε_{ij} takes different values, such as α/r^3 , $e^2/\kappa r$,

and E_H , the original Mott law,¹ the Efros and Shklovskii variable range hopping equation,² and the hard gap resistance³⁻¹² can be derived correspondingly by setting $P = 0$ in Eq. (2).

As mentioned above, $\text{Zn}_{1-x}\text{Fe}_x\text{O}_{1-v}$ films are amorphous and show compositional inhomogeneity on the subnanometer scale. The compositional inhomogeneity of the ferromagnetic semiconductor can produce not only local electrical potential but also local magnetic potential, which may result in the localization of the carriers near the Fermi level. In the Anderson localization system, the electrical transport is caused by carrier hopping from the initial localized occupied state to the final vacant state due to thermal activation. The hopping carriers should be localized s , p carriers near the Fermi level.

In the present case, the energy difference ε_{ij} between the initial occupied i state and the final vacant j state of the hopping process is determined by interactions in the $\text{Zn}_{1-x}\text{Fe}_x\text{O}_{1-v}$ magnetic semiconductor system. One of the interactions in this system is an electron-electron Coulomb interaction between two carriers, $E_{C0} = e^2/\kappa r$, where κ is the dielectric constant. On the other hand, there also exists spin-spin exchange interaction between the s , p carriers of defect levels and strongly localized d electrons of Fe, in addition to direct d - d exchange interactions between d electrons of the neighbor Fe atoms due to a high Fe concentration. Therefore, local Fe may establish a local ferromagnetic order through s , p - d [or Ruderman-Kittel-Kasuya-Yoshida (RKKY)] and d - d exchange interactions. Supposing that Hund's coupling is strong, the spin of a carrier is coupled to the spin of its nearest local Fe atom. In this case, two carriers can show an effective spin-spin exchange interaction between them through the surrounding Fe atoms which have formed local ferromagnetic order. Analogizing the RKKY interaction for a large distance in one dimension²⁵ where its magnitude is proportional to $1/r$, the effective spin-spin exchange interaction between two carriers is assumed to take the form of $E_{ex} = -(J/r)\cos \theta$, where J represents the coupling strength. It is noted that in $\text{Zn}_{1-x}\text{Fe}_x\text{O}_{1-v}$ magnetic semiconductors of high Fe content, the distance between the neighbor Fe atoms is small. However, in a low temperature range, the thermal energy may be not large enough to activate the nearest neighbor transitions. Instead, the carrier may hop a large distance to find a low hopping barrier between the initial occupied state and the final vacant state. Since the hopping distance of the Efros and Shklovskii variable range hopping is proportional to $T^{-1/2}$, the hopping distance can be large in the low temperature range. For the hopping process of large distance r from the initial occupied state to the final vacant state, the energy difference in exchange interaction may be mainly related to the spins in the hopping path. In this sense, the exchange interaction picture of one dimension is reasonable. Therefore, the effective spin-spin exchange interaction between two carriers is assumed to take a form of $E_{ex} = -(J/r)\cos \theta$, which analogizes the RKKY interaction for a large distance in one dimension. As for the hard gap energy E_H , it can be regarded as a constant in spite of its various origins.^{4,7,10}

Taking into account the interactions mentioned above,

the total energy difference between the initial occupied i state and the final vacant j state of the hopping process in the distance r is

$$\varepsilon_{ij} = E_H + \frac{e^2}{\kappa r} - \frac{J}{r} \cos \theta. \quad (3)$$

Putting Eq. (3) into Eq. (2) and finding the optimal hopping distance r at a certain temperature T to minimize the hopping resistance ρ_{ij} ,^{12,19} we get

$$\rho_{ij} = \frac{\rho_0}{1 + P^2 \cos \theta} \exp \left[\frac{T_H}{T} + \left(\frac{T_{ES}}{T} \right)^{1/2} \right], \quad (4)$$

where

$$T_H = \frac{E_H}{k_B}, \quad T_{ES} = \frac{8e^2}{\kappa k_B \xi} - \frac{8J}{k_B \xi} \cos \theta.$$

For the system, the spins of localized states may have their own local quantum easy axes, so the angle θ may have a distribution and vary with the applied magnetic field. As an approximation of the hopping resistance ρ of the system, we can use $\langle \cos \theta \rangle$ (the average of $\cos \theta$ over the whole system) to replace $\cos \theta$ in Eq. (4), i.e.,

$$\rho = \frac{\rho_0}{1 + P^2 \langle \cos \theta \rangle} \exp \left[\frac{T_H}{T} + \left(\frac{\langle T_{ES} \rangle}{T} \right)^{1/2} \right] \quad (5)$$

and

$$\langle T_{ES} \rangle = \frac{8e^2}{\kappa k_B \xi} - \frac{8J}{k_B \xi} \langle \cos \theta \rangle. \quad (6)$$

A conventional way to obtain a hopping resistance should be calculated by percolation theory, which takes into account all conducting paths with different distance r and angle θ . As an approximate expression of the hopping resistance, Eq. (5) is not strict in mathematics, but it keeps the same function form of Eq. (4). In the following paragraphs, we will see that Eq. (5) is accurate enough to describe the experimental results. Therefore, we did not give a more detailed description by percolation theory. If we further suppose that the easy axes of localized states are random in the film, we can obtain $\langle \cos \theta \rangle = m^2$, where m is the relative magnetization of the system. In particular, although there is a local spontaneous magnetization, the net magnetization of the whole system is 0 in a demagnetized state (the as-deposited film without applying any magnetic field), i.e., $\langle \cos \theta \rangle = m^2 = 0$. In a mag-

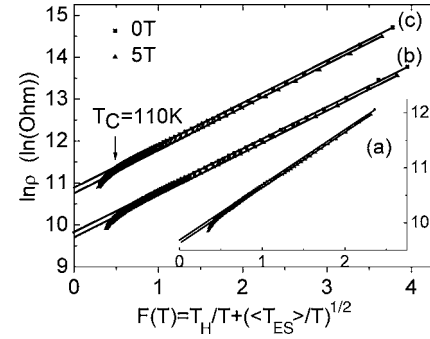


FIG. 4. The dependence of $\ln \rho$ on $F(T) = (T_H/T) + (\langle T_{ES} \rangle / T)^{1/2}$ for the three samples described in Figs. 2. The squares are the experimental results in the demagnetized state ($H=0$), the triangles are the experimental results in the saturation state ($H=5$ T), and the straight lines are the theoretical fittings according to Eq. (5). The mark T_C is a temperature below which the experimental results can be well described by Eq. (5) for given samples.

netic saturation state, all local magnetizations are along the direction of the applied field, i.e., $\langle \cos \theta \rangle = m^2 = 1$. Finally, it is worthy to mention that Eq. (1) can be directly derived from Eq. (5).

V. THEORETICAL FITTING AND DISCUSSION

Figure 4 shows theoretical fittings according to Eq. (5), which gives the dependence of $\ln \rho$ on $(T_H/T) + (\langle T_{ES} \rangle / T)^{1/2}$ for different samples. The samples marked by (a), (b), and (c) in Fig. 4, respectively, correspond to samples described in Figs. 2(a)–2(c). It is clear that $\ln \rho$ linearly depends on $(T_H/T) + (\langle T_{ES} \rangle / T)^{1/2}$ in a wide temperature range for all samples. Compared with the fittings in Figs. 2, the electrical transport of the samples can be well described by Eq. (5) in a wider temperature range, as shown in Fig. 4.

From the above theoretical fittings by Eq. (5), fitting parameters of different samples were obtained and listed in Table I. In contrast with the $\langle T_{ES} \rangle$, the E_H in Table I does not depend on the magnetic field for a given sample, which means that the E_H does not have a magnetic origin since the magnetic E_H is easily eliminated by a high applied magnetic field.^{4,5,7-9} A possible origin of the nonmagnetic E_H in $\text{Zn}_{1-x}\text{Fe}_x\text{O}_{1-v}$ magnetic semiconductors is the many-electron excitation effect as proposed in Ref. 10 for strongly localized disordered systems. According to Ref. 10, when a hop of length r occurs, the compact pairs whose excitation energy is smaller than their interaction energy with the electrical field

TABLE I. $\langle T_{ES} \rangle$, hard gap energy E_H , $8J/k_B \xi$, the absolute value of the ratio of exchange interactions to Coulomb interactions $|E_{ex}/E_{Co}|$ for $\cos \theta = 1$, and spin polarization ratio P , which were obtained from the fittings according to Eq. (5). The description of $\langle T_{ES} \rangle$ and $8J/k_B \xi$ can be found in the text. The thicknesses of the films were also shown.

$\text{Zn}_{1-x}\text{Fe}_x\text{O}_{1-v}$ x value	$\langle T_{ES} \rangle$ (K)		E_H (meV)	$8J/k_B \xi$ (K)	$ E_{ex}/E_{Co} $ (%)	P (%)	Thickness (nm)
	0 T	5 T					
0.46	412.9349	406.2530	0	6.6819	1.62	25.0	50.0
0.50	196.8126	190.3288	0	6.4838	3.29	22.3	44.4
(a) 0.70	24.9179	23.7633	0	1.1546	4.63	20.6	27.4
(b) 0.77	43.5057	39.4500	0.44	4.0557	9.32	26.9	23.6
(c) 0.86	23.1016	20.4798	0.72	2.6218	11.35	30.0	18.9

produced by transition will be polarized, especially the pairs which are near the initial state and the final state of a long range hopping. So low-energy many-electron excitations may become more significant, which leads to a hard gap in single-particle densities of states close to the Fermi energy.

According to Table I, for the samples with Fe composition no more than 70 at. %, such as $\text{Zn}_{0.3}\text{Fe}_{0.7}\text{O}_{1-v}$, $\text{Zn}_{0.5}\text{Fe}_{0.5}\text{O}_{1-v}$, and $\text{Zn}_{0.54}\text{Fe}_{0.46}\text{O}_{1-v}$, the T_H/T term is zero ($E_H=0$) and only the $(\langle T_{ES} \rangle/T)^{1/2}$ term takes a rule. Therefore, the resistance can be well described by the Efros and Shklovskii variable range hopping theory in a wide temperature range, as already shown in Fig. 2(a). For high Fe composition, for example, $\text{Zn}_{0.14}\text{Fe}_{0.86}\text{O}_{1-v}$ sample, the T_H/T term (E_H) dominates over the $(\langle T_{ES} \rangle/T)^{1/2}$ term in the low temperature range. As a result, the hard gap resistance was observed, as already shown in Fig. 2(c).

For the sample $\text{Zn}_{0.23}\text{Fe}_{0.77}\text{O}_{1-v}$, the T_H/T term and the $(\langle T_{ES} \rangle/T)^{1/2}$ term are comparable, and hence the electrical transport cannot be described only by the Efros and Shklovskii variable range hopping theory or by the hard gap law. Comparing Fig. 4 with Figs. 2 it is clear that the fitting function $\ln \rho = B + CT^\alpha$ used in Figs. 2 is just an approximation of Eq. (5) for certain samples in a narrow range of temperature. Therefore, Eq. (5) is a universal form of resistance, which can well describe the transformation of electrical transport from variable range hopping to hard gap resistance.

From Table I, the absolute value of the ratio of exchange interaction to Coulomb interaction monotonously increases with increasing Fe composition, which means that a relative contribution of exchange interaction to electrical transport increases with increasing Fe composition. The relatively strong exchange interaction may greatly enhance magnetoresistance of the system.

It is obvious that the transformation from variable range hopping to hard gap resistance in $\text{Zn}_{1-x}\text{Fe}_x\text{O}_{1-v}$ magnetic semiconductors was caused by the variation of the chemical composition. As the composition changes, the energy band structures change and hence the density of states near the Fermi energy changes, but semiconductor conducting characters are still kept for the Fe concentration x from 0.46 to 0.86. When Fe concentration is relatively low, average distance between the neighbor Fe atoms is relatively large, and electron correlation effect is weak. In this case, the experimental results of electrical transport [see Fig. 2(a)] indicate that the electrical transport can be well described by the picture of spin-dependent hopping of a single electron to create an electron-hole pair. This means that the spin-dependent variable range hopping can work well and many-electron excitation effects can be neglected.

By contrast, when Fe concentration is relatively high, average distance between the neighbor Fe atoms is relatively small, and electron correlation effects become strong. In this case, the experimental results of the electrical transport [see Figs. 2(b) and 2(c)] indicate that the electrical transport cannot be described by a simple picture of spin-dependent hopping of a single electron to create an electron-hole pair. The many-electron excitation effects which induce the hard gap energy must be taken into account. Since the short-ranged

many-electron excitation effects are induced by long-ranged single electron hopping,¹⁰ the pure hard gap transport ($E_H > 0$ and $\langle T_{ES} \rangle = 0$) does not exist in this case, as shown in Figs. 2(b) and 2(c) (or the fitting parameters in Table I). As mentioned before, the T_H/T term and the $(\langle T_{ES} \rangle/T)^{1/2}$ term are comparable in Fig. 2(b), and the T_H/T term (E_H) dominates over the $(\langle T_{ES} \rangle/T)^{1/2}$ term in Fig. 2(c) in the low temperature range. However, for the range of the experimental composition x from 0.46 to 0.86, Eq. (5) can well describe all observed magnetic transport phenomena.

However, as Fe composition increases, the $8J/k_B\xi$ value shows nonmonotonic behavior, which may be due to the sample dependent variation of the localization length ξ . This implies that further research work is needed for more understanding of spin-spin exchange interactions and electrical transport property in magnetic semiconductors.

VI. CONCLUSIONS

In summary, as Fe composition increases, the crossover behavior from the Efros and Shklovskii variable range hopping to the “hard gap” resistance was experimentally observed. A theoretical electrical transport model, which can well describe the experimentally observed transport phenomena, was established by taking into account electron-electron Coulomb interaction, spin-spin exchange interaction, and hard gap energy. Fitting the theoretical model to the experimental results, spin polarization ratio, hard gap energy, and ratio of exchange interactions to Coulomb interactions were obtained.

ACKNOWLEDGMENTS

This work was supported by the State Key Project of Fundamental Research of China, Grant No. 2001CB610603, NSF Grant Nos. 10234010, 50402019, and 50572053, and NCET040634.

- ¹N. F. Mott, *J. Non-Cryst. Solids* **1**, 1 (1968).
- ²A. L. Efros and B. I. Shklovskii, *J. Phys. C* **8**, L49 (1975).
- ³J.-J. Kim and H.J. Lee, *Phys. Rev. Lett.* **70**, 2798 (1993).
- ⁴I. Terry, T. Penney, S. von Molnár, and P. Becla, *Phys. Rev. Lett.* **69**, 1800 (1992).
- ⁵A. I. Yakimov, T. Wright, C. J. Adkins, and A. V. Dvurechenskii, *Phys. Rev. B* **51**, 16549 (1995).
- ⁶A. S. Ioselevich, *Phys. Rev. Lett.* **71**, 1067 (1993).
- ⁷P. Dai, Y. Zhang, and M. P. Sarachik, *Phys. Rev. Lett.* **69**, 1804 (1992).
- ⁸W. N. Shafarman, D. W. Koon, and T. G. Castner, *Phys. Rev. B* **40**, 1216 (1989).
- ⁹R. Oppermann and B. Rosenow, *Phys. Rev. Lett.* **80**, 4767 (1998).
- ¹⁰R. Chicon, M. Ortuño, and M. Pollak, *Phys. Rev. B* **37**, 10520 (1988).
- ¹¹T. Sato, K. Ohashi, H. Sugai, T. Sumi, K. Haruna, H. Maeta, N. Matsu-moto, and H. Otsuka, *Phys. Rev. B* **61**, 12970 (2000).
- ¹²A. N. Aleshin, A. N. Ionov, R. V. Parfen'ev, I. S. Shlimak, A. Heinrich, J. Schumann, and D. Elefant, *Fiz. Tverd. Tela (Leningrad)* **30**, 696 (1988) [*Sov. Phys. Solid State* **30**, 398 (1988)].
- ¹³Y. Meir, *Europhys. Lett.* **33**, 471 (1996).
- ¹⁴H. Kamimura, A. Kurobe, and T. Takemori, *Physica B & C* **117**, 652 (1983).
- ¹⁵I. Shlimak, S. I. Khondaker, M. Pepper, and D. A. Ritchie, *Phys. Rev. B* **61**, 7253 (2000).
- ¹⁶S. von Molnár, A. Briggs, J. Flouquet, and G. Remenyi, *Phys. Rev. Lett.* **51**, 706 (1983).
- ¹⁷A. Oiwa *et al.*, *Phys. Status Solidi B* **205**, 167 (1998).
- ¹⁸P. Wagner, I. Gordon, L. Trappeniens, J. Vanacken, F. Herlach, V. V.

- Moshchalkov, and Y. Bruynseraede, Phys. Rev. Lett. **81**, 3980 (1998).
- ¹⁹M. Viret, L. Ranno, and J. M. D. Coey, Phys. Rev. B **55**, 8067 (1997).
- ²⁰P. Xiong, B. L. Zink, S. I. Applebaum, F. Hellman, and R. C. Dynes, Phys. Rev. B **59**, R3929 (1999).
- ²¹S.-s. Yan *et al.*, Appl. Phys. Lett. **84**, 2376 (2004).
- ²²V. Ambegaokar, B. I. Halperin, and J. S. Langer, Phys. Rev. B **4**, 2612 (1971).
- ²³J. Inoue and S. Maekawa, Phys. Rev. B **53**, R11927 (1996).
- ²⁴S. Ju and Z.-Y. Li, J. Appl. Phys. **92**, 5281 (2002).
- ²⁵T. Dietl, A. Haury, and Y. M. d'Aubigné, Phys. Rev. B **55**, R3347 (1997).